



Thermal Optimisation of e-Drives Using Moving Particle Semi-implicit (MPS) Method



Abstract: A novel technique to model the temperature of windings in oil cooled e-machines has been developed. It aims to reduce the time taken to generate and solve thermal models by using a combination of particle based fluid modelling and steady state finite element (FE) thermal modelling. The fluid model is used to generate a heat transfer coefficient (HTC) map for the complex, multi-phase flow, which is applied to a finite element FE model of the e-machine. This would allow thermal modelling to take place at a concept design stage where rapid design iterations are required.

By using this combined modelling approach, it was shown that it is possible to generate and solve models in under a week which show credible results. Further correlation work is underway to validate the models and results predicted.

Keywords: MPS, e-machine thermal modelling, oil cooled e-machine, multi-phase flow.

1. Introduction

With major OEMs committing to increasing numbers of EVs and greater electrification, the total electric car stock could reach between 9 million and 20 million by 2020 (4). To make this possible, the UK's Advanced Propulsion Centre (APC) have outlined target costs, power

Passenger Car Traction Motor ¹	2017	2025	2035
Cost (\$/kW) ²	10	5.8	4.5
Continuous power density (kW/kg)	2.5	7	9
Continuous power density (kW/l)	7	25	30
Drive cycle efficiency (%) ³	86.5	92.5	93

1) All assume 350V / 450Amps @ 65degC inlet

2) Prices are 300% mark-up on material costs

3) Drive cycle based on WLTP

Figure 1: APC Targets for Passenger Car Traction Motors (5)

densities and efficiencies for passenger vehicle traction e-machines, as shown in Figure 1 (5).

They also note that one key technological enabler is the closer integration of e-machines into transmissions and internal combustion engines (ICEs), and eventually fully integrated powertrains. This means that there will be a shared cooling and lubrication strategy within the transmission and e-machine, tending towards oil cooled e-machines. A passive (splash) lubrication regime is likely to maximise the efficiency of the integrated powertrain whilst minimising cost and weight but may not deliver sufficient cooling for high power density e-machines. Down-sized, low power electric pumps will be required to balance efficiency, mass and cooling.

With increasing power density motors, the loss density will also increase, meaning that more effective e-machine cooling will be required. Alongside more integration in powertrains, e-machine cooling becomes a factor in the lubrication design and it will become increasingly necessary to use fluid modelling to influence concept level designs.

Currently it is difficult to accurately model fluid flow within enclosed volumes such as transmissions and e-machines with traditional computational fluid dynamics (CFD) methods due to the high computation time required. It is even less practical to model heat dissipation as the bulk temperature stabilises over a much greater timescales than the fluid flow, meaning even greater computation time is required. As a result, it is currently impractical to perform in the early stages of a new design where rapid iterations are required. This is currently a barrier at the concept stage to the optimisation of oil cooled e-machines.

It has been shown that modelling oil within enclosed volumes with rotating components, such as transmissions, can be performed effectively on modest hardware (2) (6). This paper builds on this work to model multiphase fluid flow within an oil cooled e-machine.

By combining this approach with FE it is possible to model the temperature distribution in the windings of an oil cooled e-machine in a compressed timescale, enabling faster design iterations and more power dense e-machines through thermal optimisation.

2. Thermal Modelling

2.1 Modelling Oil Within Powertrains

To understand the movement of oil within powertrains there are two established methods which are practiced:

- Clear case testing
- Finite volume computational fluid dynamics (CFD) modelling

Baffles, oil guides and pumps can be tested in clear cases to optimise the oil distribution. High temperature testing is not possible however due to the limitations of the materials used for clear casings - typically transparent thermoplastics such as acrylic. The clear case testing is useful once a design has matured to the extent that the rotating components are relatively well defined but cannot provide useful data during the concept design phase. It can take several months to procure rotating components and so there is often a requirement to commit to a design for clear case testing at the same time as procuring prototype test components. As such, if any significant issue is found during clear case testing there is a large cost, both in lost time and wasted material, associated with re-design and re-testing.

Finite volume CFD is of limited benefit in the design of automotive transmissions or electrified powertrains due to the extended run time required to generate results. Typically it can take several weeks of computation to generate a few seconds of real world data. Fluid flow will tend to stabilise within a few seconds in a powertrain but it may take several minutes to reach thermal steady state (6). This could require months of simulation. As multiple input speeds would need to be modelled, it rapidly becomes impractical to use this type of CFD to model a single concept even on computers with high processing power.

An increasingly well correlated alternative method of CFD using particles is more suited to modelling fluids in confined volumes (2). This meshless CFD utilises a moving particle semi-implicit (MPS) method which allows simulation of single phase and multiphase fluid flow. With MPS the fluid is discretised as a series of particles whose interactions are calculated using conservation of momentum and mass. The Navier-Stokes equations are solved using the Lagrangian methodology (6). The MPS method is able to account for surface tension, droplet break up, free surface fragmentation and coalescence. Solid bodies are represented by mathematical functions, called distance functions, and so a mesh is not required. The MPS solver can be run on graphics processing units (GPUs) to further reduce computation time. This method enables much faster solving of fluid models, for example it can take as little as a few days to simulate several seconds of real time data for a single speed automotive transmission on modest hardware, compared to weeks using finite volume CFD.

Figure 2 shows a comparison of MPS vs CFD solve times for a simple automotive transmission. By combining the performance benefits of MPS with appropriate modelling simplifications, it may be possible to use this method as an iterative design tool, rather than a final validation.

	Moving Particle Simulation	Mesh-Based CFD
Pre-process (geometry, meshing, setup)	< 1 day	2 weeks
CPU Time	5.0 [s] in 3 days	0.5 [s] in 4 weeks
Cores	12	32
GPU Time	5.0 [s] in 6 hours - v6 on K40 5.0 [s] in 3 hours - v6 on P100	

Figure 2: Comparison of MPS and CFD solve times for a simple automotive transmission (6)

2.2 Modelling Heat Transfer in Oil Cooled Motors

E-machine design software enables rapid iterations to develop high power density designs, with information on power curves and efficiency. A critical factor in increasing the power density of an e-machine is how much of the heat generated can be removed. Overheating can cause damage to the insulation and lead to short circuiting. The design of the cooling system will directly impact how much power the e-machine can produce in both continuous running and peak conditions.

There are several widely acknowledged and utilised methods for cooling E-machines in automotive transmissions:

- Water/glycol cooling jacket
- Direct oil spray onto the stator windings
- Oil or water/glycol in a hollow rotor shaft

The cooling effect of a water/glycol jacket can be calculated relatively easily as the channels are fully filled with water/glycol only. This means that correlations to empirical data is known to be accurate.

Oil sprayed directly onto the stator windings provides a greater challenge as the oil mixes with air in varying proportions over the entire surface of the windings. Empirical data is used to correlate to, however this is always a compromise as the data is inherently discontinuous, having been measured at a series of discrete points. As a result, the designs generated may not be as optimised as possible. By developing a more detailed method of modelling the temperatures on the surface of the e-machine windings it will be possible to increase its power density.

An MPS CFD method can be used to simulate the complex flow of the oil around the e-machine windings. From this it is possible to export the heat transfer coefficients (HTC). This can then be combined with the power loss in the windings to model the temperature at the surface and give indications of poorly cooled areas.

2.3 Motor Design and Cooling Strategy

A high power density e-machine has been developed by DSD for an automotive application using state of the art e-machine design software. Initially a winding temperature prediction was carried out using correlation to empirical data. The data showed a step change in temperature under certain conditions which is due to the discrete nature of the empirical data.

The design, Figure 3, uses a series of spray cooling jets to introduce oil onto the windings, which then drains down into a remote sump (not shown) allowing the oil to settle and de-aerate. An oil to air radiator is used to cool the oil before it reaches the e-machine.

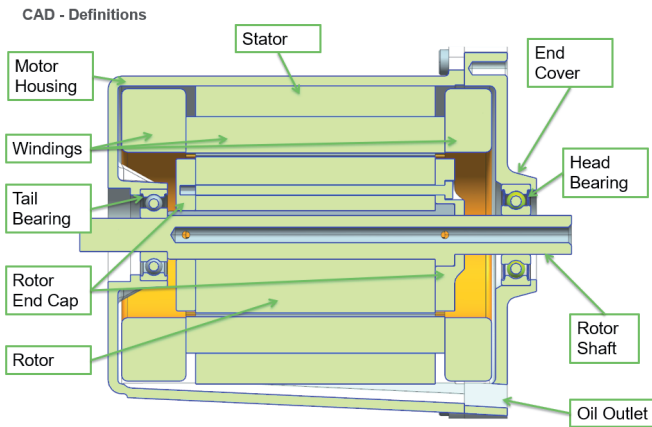


Figure 3: e-machine Design

A single oil spray nozzle feeds oil to each end of the windings from the highest point on the casing. A nozzle also feeds oil directly up the centre of the rotor shaft, with four radial drillings spreading this oil to the inside of the windings. The pump selected for this design is capable of supplying 8L/min of oil to the e-machine. An initial estimate of the required flow rate split is shown in Figure 4.

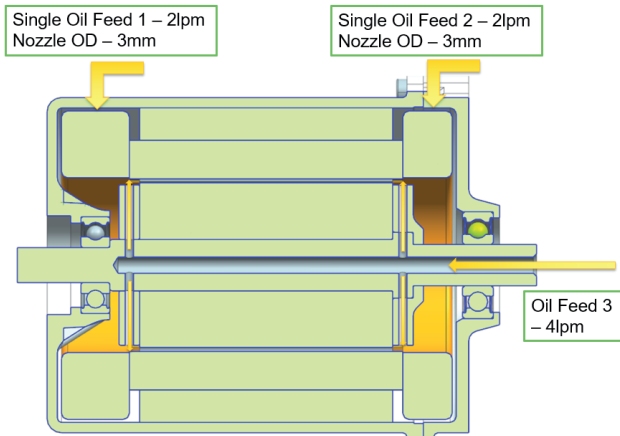


Figure 4: Initial Oil Requirements

This e-machine is required to run at the continuous high power and building an analytical model offers the opportunity to test the estimated oil cooling and optimise the cooling regime.

2.4 Modelling the System

It has previously been shown how the flow of oil using an MPS method can be correlated to test data (6). Figure 5 shows the model used in this test.

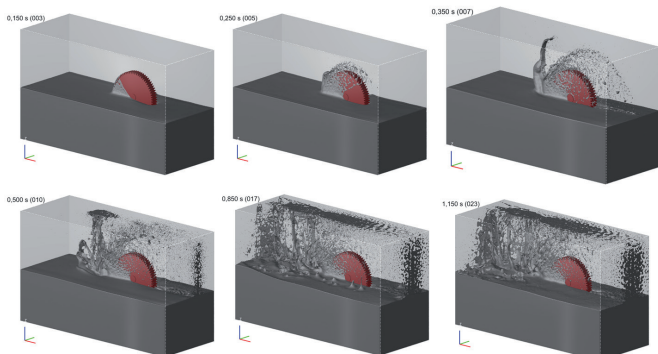


Figure 5: Correlation model of single gear in oil (6)

For the e-machine analysis a model was generated in Particleworks, using imported CAD. The solid components were imported as grouped bodies based on how they will behave within the model. The rotor was combined with the bearing inner races and elements into a single body as these will all rotate about the same axis (Figure 6) to reduce pre-processing time.

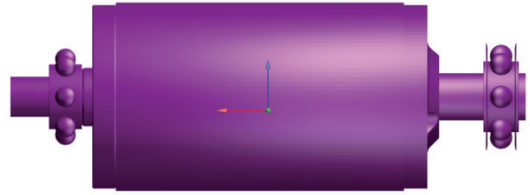


Figure 6: Rotating Components

The stator and windings were imported as separate bodies so that information such as heat transfer coefficients could be investigated for these components individually (Figure 7).

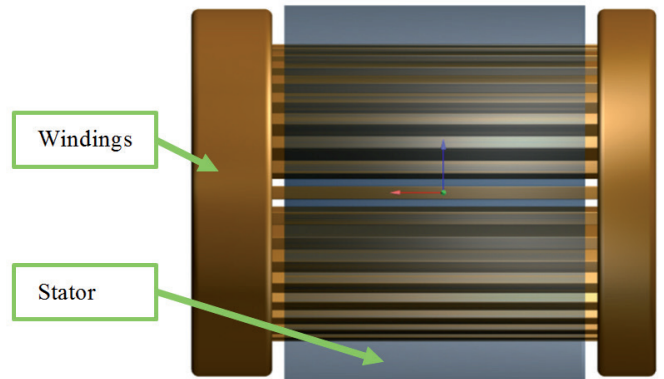


Figure 7: Stationary Components

The inner surface of the casing, including the bearing outer races, was extracted to create an oil tight containment volume, with the outer surface simplified to a cube (Figure 8). This simplification was carried out to reduce the pre-processing time required to generate the distance functions for the solid body.

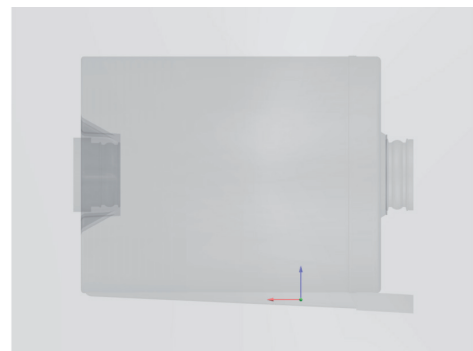


Figure 8: Containment Volume

An initial model was generated which isolated the rotor assembly to calculate the oil flow through the radial drillings. The rotor shaft was placed within a cubic domain with an oil feed into the centre of the shaft. The rotor was set to rotate at 3000RPM, with the oil fed at a rate of 4L/min.

Once the flow had become stable, the flow rate from each orifice was measured as shown in Table 1. Figure 9 shows the rotor shaft before

Orifice	Flow Rate (L/min)	Percentage
Inlet	4	100
Outlet 1	1.0109	25.27
Outlet 2	1.0096	25.24
Outlet 3	0.9896	24.74
Outlet 4	0.9899	24.75

Table 1: Flow Rate at Inlet and Outlets

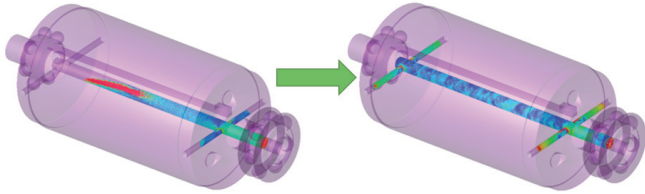


Figure 9: Oil Flow Through Rotor Shaft

flow had stabilised and after flow had stabilised and the rotor becomes saturated.

As the flow rate of each orifice is approximately equal, a fixed flow rate equal to one quarter of the input flow will be used at each orifice in the complete model to reduce the computation time required to solve.

A complete model was generated, including the modelling simplification described above. For low speed applications it is possible to model an enclosed volume without air to significantly decrease the computation time required. As the tip speed on the rotor shaft is between high

speed and low speed, back to back models were generated with and without air to determine whether it was necessary. Figure 10 shows the development of the oil flow in the model without air, coloured by velocity. The model shows, in the circled region, areas where oil doesn't appear to reach.

Figure 11 shows the oil and air flow developing in the model with air, the air particles are coloured pink throughout whilst the oil is coloured by velocity.

From the test described above, it was deemed that the model with air would provide a more accurate model of the fluid movement and hence the HTC. A comparison of the HTC map for the models without and with air is shown in Figure 12 and Figure 13. It can be seen that in the model without air the HTC is very low in the areas where oil isn't reaching in significant quantities. This is to be expected as the model

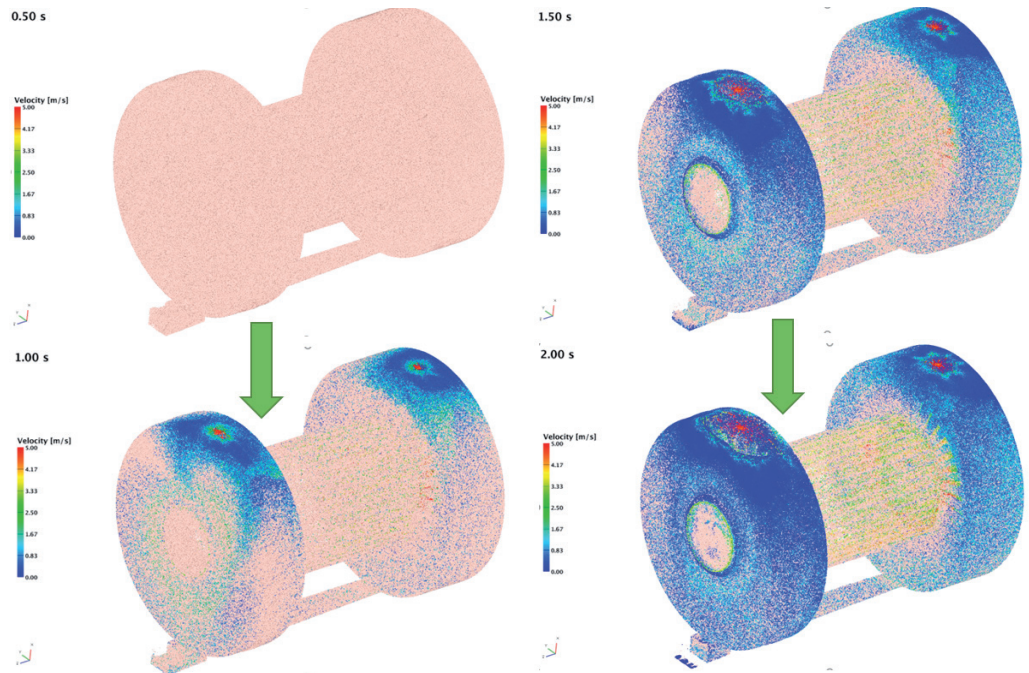


Figure 11: Development of Oil Flow (With Air)

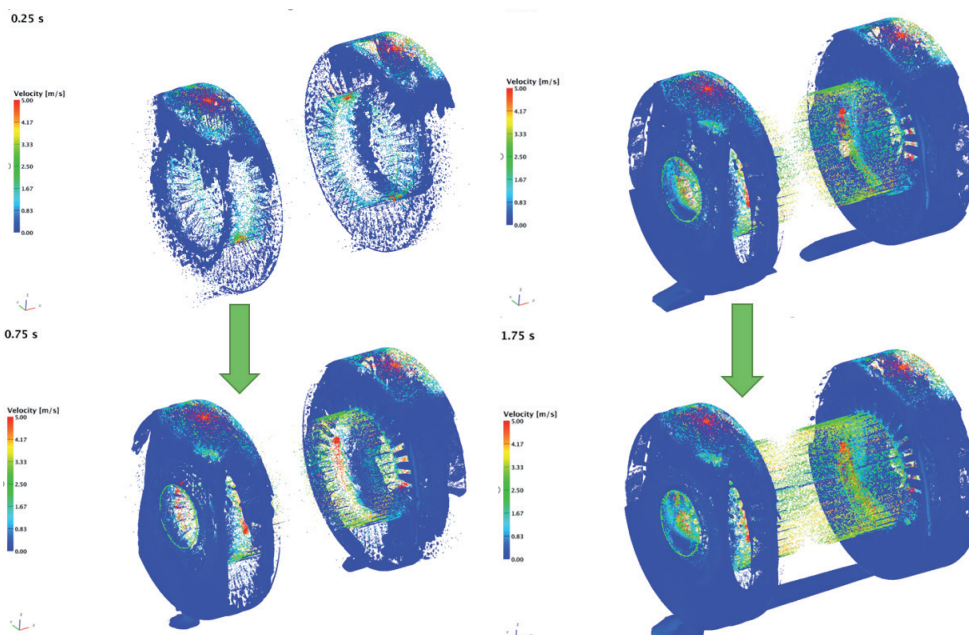


Figure 10: Development of Oil Flow (Without Air)

assumes a vacuum where there isn't oil. The model with air shows a more even distribution of HTC. This aligns with expectation well as the air will be dragged around as the rotor spins, meaning that it will also have a cooling effect on the windings. Although it would reduce computation time further, it was deemed that modelling without air would not produce reliable results.

To check whether these results fall within the expected range, a hand calculation was performed using the Dittus-Boelter Correlation at the point of the top inlet. The HTC predicted at this point by hand calculation is within 10% of the HTC predicted by the model.

3.92 s

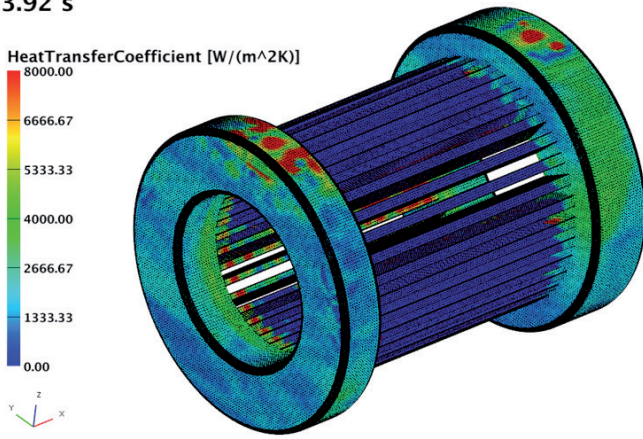


Figure 12: HTC Map (Without Air)

3.17 s

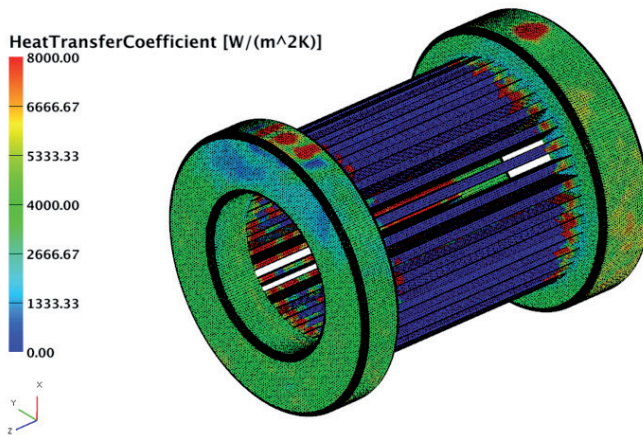


Figure 13: HTC Map (With Air)

2.5 Temperature Mapping

The HTC map was exported from the model once the flow field had stabilised. This was then mapped onto a solid mesh in FE software. The power loss predicted in the windings, from the motor design software, was applied to the windings as a volumetric power loss. Whilst the losses vary over very short distances, for the purpose of developing a simplified design tool it was assumed that the power loss is equal across the windings. This simplification will help to minimise set up time for the thermal models.

It is impractical to model each individual wire in the motor windings at a concept level, especially when these are to be analysed using FE. The insulation is very thin and would require a very fine mesh to capture correctly, greatly increasing the number of elements in the model. This would require an impractically large amount of computation time to solve (7) (8).

A method for estimating the bulk properties of a homogenised winding material has been validated by Simpson et al. (7). The effective thermal conductivity, k_e , of the winding material can be estimated using the Hashkin and Shtrickman approximation:

$$k_e = k_p \frac{(1 + v_c)k_c + (1 - v_c)k_p}{(1 - v_c)k_c + (1 + v_c)k_p}$$

Equation 1: Hashkin & Shtrickman Approximation

Where k denotes thermal conductivity, v denotes volumetric ratio with $v_c + v_p = 1$, and the subscripts e denotes effective, c denotes conductor and p denotes potting compound. The effective specific heat capacity, c_e , of the bulk material can be estimated using:

$$c_e = \frac{PF(\rho_c c_c - \rho_p c_p) + \rho_p c_p}{PF(\rho_c - \rho_p) + \rho_p}$$

Equation 2: Specific Heat Capacity Estimation

Where c , ρ , and PF denote specific heat capacity, density and packing factor respectively. The subscripts c and p denote conductor and potting compound respectively. By applying these homogenised properties to the winding, the FE model can be significantly simplified with a small reduction in accuracy (7).

A steady state heat transfer problem was then carried out using the FE solver.

3. Results

The results from the steady state heat transfer problem are shown in Figure 14. The results show low temperatures in the expected areas, the areas where the oil inlets are situated are effectively cooled by the direct jets. The inner surface of the end windings also shows a well defined region of lower temperature where the rotor shaft oil feed exits.

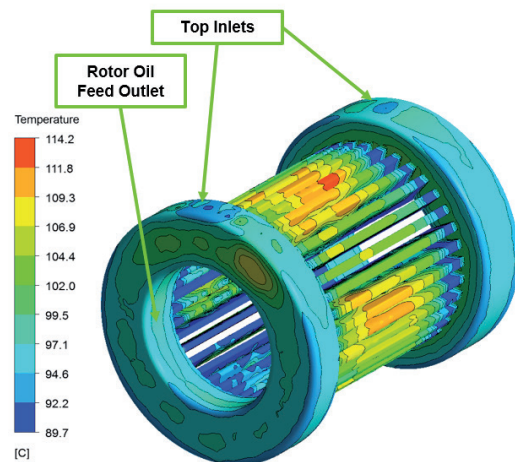


Figure 14: Temperature Map (4L/min in Rotor Shaft)

The windings which are situated within the stator show a higher temperature due to the lack of oil in this area (Figure 15). Whilst this

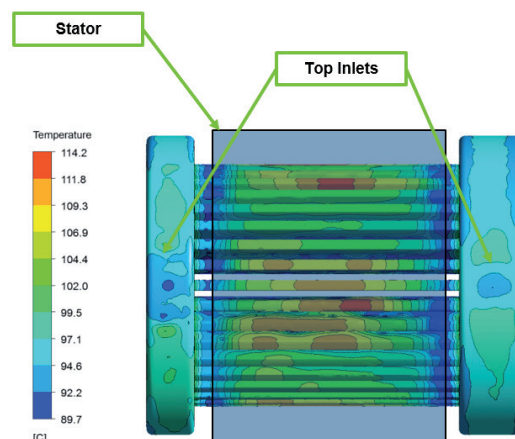


Figure 15: Temperature Map (4L/min in Rotor Shaft) Viewed From Above

is expected due to the relatively low convective heat transfer in this area, the temperature may be lower in reality as there would be heat conduction through the stator which has not been accounted for.

The peak temperature is 124.9°C, found in the centre of windings (Figure 16) whilst the average temperature across the entire windings is 103.6°C.

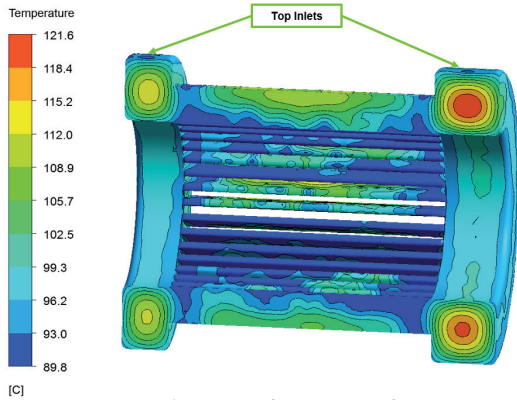


Figure 16: Temperature Map (4L/min in Rotor Shaft) Viewed in Section

The model was iterated using different flow rates in each area to test whether further optimisation was possible with the current package and pump restrictions. The additional test points are summarised in Table 2.

Model Name	Oil in rotor shaft (L/min)	Oil in each top inlet (L/min)	Total oil in (L/min)
A	4	2	8
B	6	1	8
C	2	3	8

Table 1: Flow Rate at Inlet and Outlets

Model B shows a similar pattern of temperature distribution to model A (Figure 17) but with generally slightly lower temperatures across the end windings.

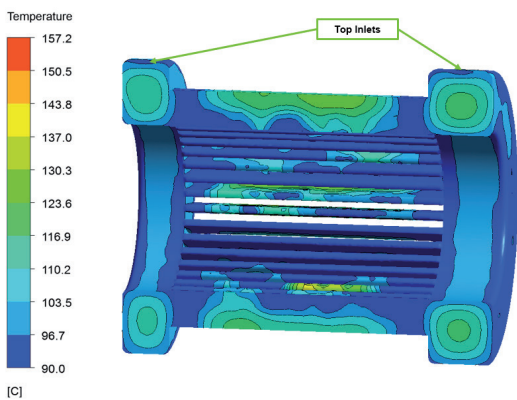


Figure 17: Temperature Map (6L/min in Rotor Shaft)

As with model A, high temperatures are seen in the area covered by the stator (Figure 18).

The peak temperature is 145.0°C, found in a very localised area in the section of windings covered by the stator (Figure 19) whilst the average temperature across the entire windings is 105.1°C.

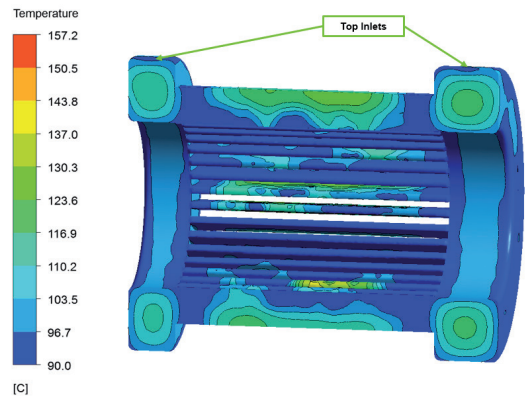


Figure 19: Temperature Map (6L/min in Rotor Shaft) Viewed in Section

Model C also shows a similar temperature distribution to models A and B (shown in Figure 20)

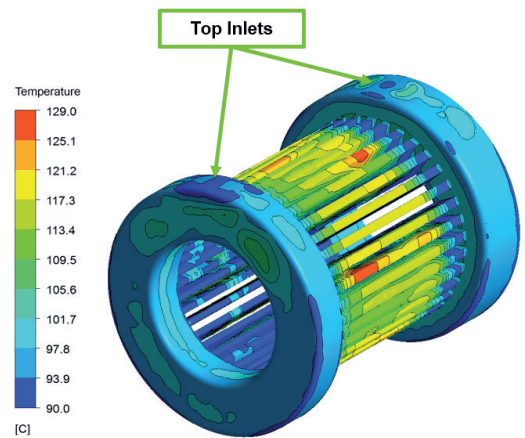


Figure 20: Temperature Map (2L/min in Rotor Shaft)

Again, the windings show high temperatures in the area covered by the stator (Figure 21).

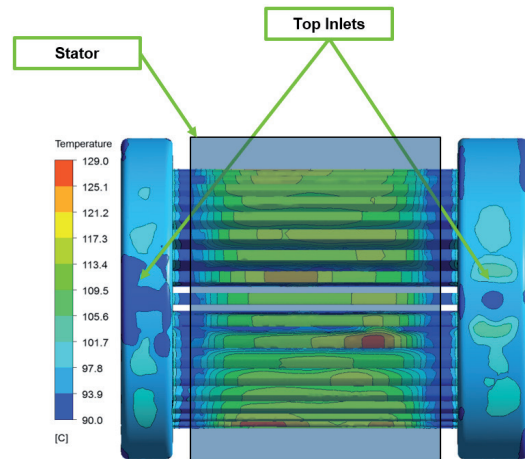


Figure 21: Temperature Map (2L/min in Rotor Shaft) Viewed From Above

In section view, it can be seen that in model C the highest temperature is found in the centre of the windings (Figure 22). The peak temperature is 129.0°C, whilst the average temperature across the entire windings is 105.0°C. The temperatures predicted by the standard motor design software for the same conditions as model A are shown in Table 3 along with the temperatures predicted using this novel method.

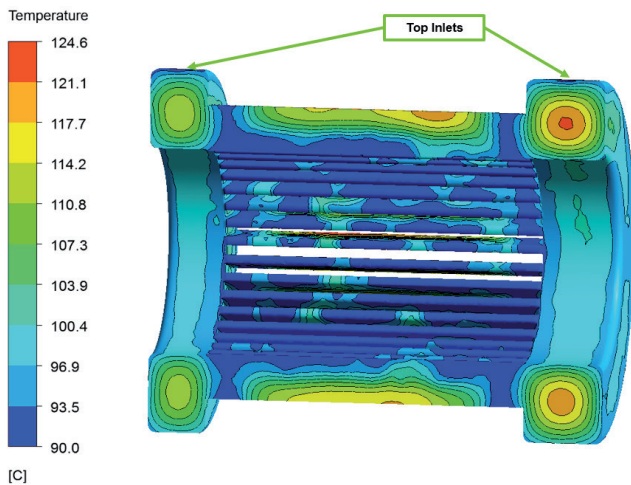


Figure 22: Temperature Map (2L/min in Rotor Shaft) Viewed in Section

Model	Peak Temp (°C)	Avg Temp (°C)
A	124.9	103.9
B	145.0	105.1
C	129.0	105.0
Standard Motor Design Software (Model A)	122.0	115.6

Table 3: Summary of Model Results

Model A, the initial estimation of flow requirements, appears to give the lowest peak temperature and lowest average temperature across the windings. This aligns with the expected trend from hand calculations. The peak temperature predicted is very similar to the standard motor design software, <2.5% difference. The average temperature predicted shows a larger difference, ~10%.

Each MPS model was set up in under half a day, with approx. 3 days of solve time on modest computer hardware. A further day was required to postprocess and solve the steady state heat transfer. This means that a set of results can be obtained in under 1 week, much less than traditional finite volume CFD techniques.

4. Conclusions

A new method for solving the heat transfer prediction problem in an e-machine has been shown. The results have been benchmarked against other existing techniques.

A suitable assumption to merge the end windings into an equivalent mass has been carried out for the purpose of this concept study. For detailed motor analysis it is feasible to model the individual end windings, however this is at the expense of computation time. It is deemed that one inaccuracy in the models is the absence of conductivity to the stator. This is currently planned to be included in the model.

As the time taken to set up and solve the model is under 1 week, this technique offers a credible method to predict temperature at the early design stage. This will allow for a more informed comparison of different designs, enabling greater optimisation of e-machine thermal performance.

Machine testing is planned during 2018 to correlate models, and refine the process.

5. Glossary

- APC: Advanced Propulsion Centre
- CFD: Computational Fluid Dynamics
- EV: Electric Vehicles
- FE/FEA: Finite Element (Analysis)
- GPU: Graphical Processing Unit
- HTC: Heat Transfer Coefficient
- ICE: Internal Combustion Engine
- MPS: Moving Particle Semi-Implicit (method)
- OEM: Original Equipment Manufacturer

References

1. International Council On Clean Transportation. EU CO2 Emission Standards For Passenger Cars And Light-Commercial Vehicles. [Online] January 2014. [Cited: 28 March 2018.] https://www.theicct.org/sites/default/files/publications/ICCTupdate_EU-95gram_jan2014.pdf.
2. Low cost, Low drag passive lubrication system developed with smoothed particle hydrodynamics. Hole, Matt. Berlin : CTI Symposium Automotive Transmissions, HEV and EV Drives, 2017.
3. Block, David and Brooker, Paul. 2015 Electric Vehicle Market Summary and Barriers. [Online] 30 July 2016. [Cited: 28 March 2018.] <http://www.fsec.ucf.edu/en/publications/pdf/FSEC-CR-2027-16.pdf>.
4. International Energy Agency. Global EV Outlook 2017. [Online] 2017. [Cited: 28 March 2018.] <https://www.iea.org/publications/freepublications/publication/GlobalEVOutlook2017.pdf>.
5. Advanced Propulsion Centre UK. APC Electric Machines Roadmap. <http://www.apcuk.co.uk>. [Online] December 2017. [Cited: 03 April 2018.] http://www.apcuk.co.uk/wp-content/uploads/2017/12/EMC_Full_Pack.pdf.
6. Galbiati, Massimo. Oil Splashing, Lubrication and Churning Losses Prediction by Moving Particle Simulation. NAFEMS World Conference 2017. [Online] June 2017. [Cited: 07 April 2018.] https://www.nafems.org/congress/presentation_downloads/.
7. Estimation of Equivalent Thermal Parameters of Electrical Windings. Simpson, N, Mellor, P H and Wrobel, R.
8. Estimation of Equivalent Thermal Conductivity for Impregnated Electrical Windings Formed from Profiled Rectangular Conductors. Ayat, S, et al.

L. Martinelli, M. Hole
Drive System Design Ltd

D. Pesenti, M. Galbiati
EnginSoft